CHEMICAL SENSORS AND CHEMICAL SENSOR SYSTEMS: FUNDAMENTALS LIMITATIONS AND NEW TRENDS

Andrea Orsini, Arnaldo D'Amico
University of Roma "Tor Vergata"
Dept. of Electronic Engineer, Via del Politecnico, 1 00133 Roma
andrea.orsini@psm.rm.cnr.it, damico@eln.uniroma2.it

Abstract

Chemical sensors are becoming more and more important in any area where the measurement of concentrations of volatile compounds is relevant for both control and analytical purposes. They have also found many applications in sensor systems called electronic noses and tongues.

This chapter will first consider fundamentals of sensor science including a brief discussion on the main terms encountered in practical applications, such as: sensor, transducer, response curve, differential sensitivity, noise, resolution and drift.

Basic electronic circuits employed in the sensor area will be discussed with a particular emphasis on the noise aspects, which are important for achieving high resolution values in those contexts where measurement of the lowest concentration values of chemicals is the main objective.

All the most relevant transducers such as: MOSFET, CMOS, Surface Plasmon Resonance device, Optical Fibre, ISFET, will be covered in some detail including their intrinsic operating mechanisms and showing their limitation and performance. Shrinking effects of these transducers will also be commented on.

The electronic nose and electronic tongue will be described as systems able to give olfactory and chemical images, respectively, in a variety of applications fields, including medicine, environment, food and agriculture.

Finally some future trends will be outlined in order to predict possible applications derived from today's micro and nanotechnology developments.

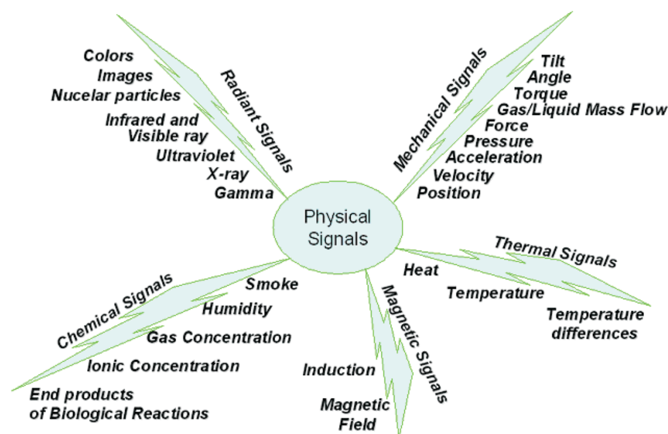

Figure 1. Signal Domains and Parameters.

1. Introduction–Parameters

In the course of the last twenty years, using techniques borrowed from standard silicon technology, silicon sensors became fundamental for the measurement of most physical and chemical parameters. Figure 1 shows the physical domains and the parameters for which silicon sensors have been introduced.

In the case of chemically sensitive devices, the interaction of a given volatile compound or ions in solution can produce one of the following changes: mass, charge, temperature, refractive index, magnetic field, work function. For each of these changes suitable transducers are now available.

Generally speaking sensors are devices able to interface the chemical, physical and biological world with that of electronics and /or electro - optics for processing, storing, communications and data presentation. In the following we introduce the most important sensor parameters and review the most successful chemical sensors able to reveal mass, charge and refractive index variations due to absorption-desorption processes involving volatile compounds.

Response Curve

The response curve (RC) represents the calibrated output response of a sensor as a function of the measurand/s applied to its input. For instance, in the case of a chemical sensor based on conductivity (G), it is recommended to use one of the following notations [1] for the output response:

- G (*conductance*);
- G/G_0 (*relative conductance*);
- ($G - G_0$) (*conductance change*);
- $(G - G_0)/G_0$ (*relative conductance change*).

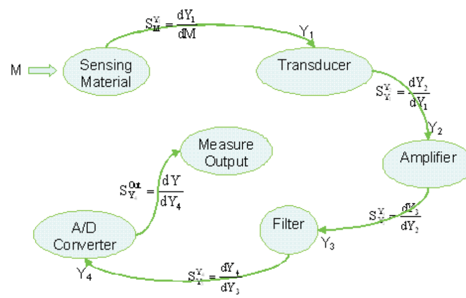

Figure 2. A complex Sensor

In the case of a sensor whose output is a frequency, the representations of the output responses may be as follows:

- f (*frequency*);
- f/f_0 (*relative frequency*);
- ($f - f_0$) (*frequency change*);
- $(f - f_0)/f_0$ (*relative frequency change*).

It is worth mentioning that for the communication of useful information the operating point of the sensors must always be specified in terms of sensor temperature, electrical or magnetic polarization, and number of fundamental blocks of the sensor model (figure 2).

Sensitivity

Sensitivity (S) is defined as the derivative of the response (as a function of the operating point) with respect to the measurand (M) and, with reference to the four cases above, we have:

- $S = dG / dM$;
- $S = d(G/G_0) / dM$;
- $S = d(G - G_0) / dM$;

- $S = d(G - G_0)/G_0 / dM$.

In the case of a linear response without offset, the previous sensitivity relationships simplify to:

LINEAR RESPONSE	
Conductivity Based Sensor	Frequency Output Sensors
■ $S = G / M$; ■ $S = (G/G_0) / M$; ■ $S = (G - G_0) / M$; ■ $S = (G - G_0)/G_0 / M$.	■ $S = f / M$; ■ $S = (f/f_0) / M$; ■ $S = (f - f_0) / M$; ■ $S = (f - f_0)/f_0 / M$.

In the case of a piecewise linear response, for each of the segments the sensitivities can be simplified as follows:

PIECEWISE LINEAR RESPONSE	
Conductivity Based Sensor	Frequency Output Sensors
■ $S = \Delta G / \Delta M$; ■ $S = \Delta(G/G_0) / \Delta M$; ■ $S = \Delta(G - G_0) / \Delta M$; ■ $S = \Delta(G - G_0)/G_0 / \Delta M$.	■ $S = \Delta f / \Delta M$; ■ $S = \Delta(f/f_0) / \Delta M$; ■ $S = \Delta(f - f_0) / \Delta M$; ■ $S = \Delta(f - f_0)/f_0 / \Delta M$.

With reference to fig. 2 we define the different sensitivities as follows:

- ${}^{i}S = \frac{dY_1}{dM}$ Internal S
- ${}^{T}S = \frac{dY_2}{dY_1}$ Transduction S
- ${}^{A}S = \frac{dY_3}{dY_2}$ I, V, G, R Amplifier S
- ${}^{F}S = \frac{dY_4}{dY_3}$ Filter S
- ${}^{A/D}S = \frac{dY_{OUT}}{dY_4}$ Analog/Digital Conversion S
- ${}^{T}S_0 = \frac{dY_2}{dY_1} * \frac{dY_1}{dM} = \frac{dY_2}{dM}$ Overall Transduction S
- ${}^{A}S_0 = \frac{dY_3}{dY_2} * \frac{dY_2}{dY_1} * \frac{dY_1}{dM} = \frac{dY_3}{dM}$ Overall Amplifier S
- ${}^{F}S_0 = \frac{dY_4}{dY_3} * \frac{dY_3}{dY_2} * \frac{dY_2}{dY_1} * \frac{dY_1}{dM} = \frac{dY_4}{dM}$ Overall Filter S

- $^{A/D}S_0 = \frac{dY_{OUT}}{dY_4} * \frac{dY_4}{dY_3} * \frac{dY_3}{dY_2} * \frac{dY_2}{dY_1} * \frac{dY_1}{dM} = \frac{dY_{OUT}}{dM}$ Overall A/D S

We apply some of the above definitions to practical examples related to temperature and chemical sensors.

Noise (N)

Resolution can only be determined after noise evaluation of the sensor, keeping in mind that noise is related to the operating point. In practical situations different kinds of noises can be encountered: Thermal, Flicker, Generation–Recombination, Shot, and others that are seen in special cases but are not so frequent. The most important parameter used for the characterization of noise devices is the Noise Spectral Density by which, through integration, it is possible to estimate the mean square value of the output voltage:

$$V^2 = \int_{f_{low}}^{f_{high}} S(f) \cdot df \tag{1}$$

where:

- S(f) = 4 k T R for thermal noise,
- S(f) = 2 q I for shot noise,
- S(f) = k V^2/f^{α} with α close to 1 for flicker noise and
- S(f) = k_1 k_2 / $(1+w^2\tau^2)$ for g-r noise.

Resolution

At the theoretical level resolution (R) is defined as the amount of the measurand which gives a signal to noise ratio equal to one at the output and can be expressed, in a simplified form, as:

$$R = (NoiseVoltage)/S. \tag{2}$$

In practice it is defined as the amount of the measurand which gives a signal to noise ratio equal to 3 or 6 or 9, according to the kind of application, at the output and can be expressed in a simplified form as:

$$R = (3 \quad or \quad 6 \quad or \quad 9) * (Noise \quad Voltage)/S, \tag{3}$$

which means, in all cases, that sensors showing the same output noise present the better solution when *Sensitivity* is higher. Since sensitivity is a function of the operating point, so is resolution.

Resolution can be defined in two other ways: minimum detectable signal level applicable when the response is in the vicinity of the output noise level, and minimum detectable signal change level applicable at any operating point along the domain of the response curve when the measurand change is close to the noise level.

Drift

Drift (D) represents a slow, unpredictable fluctuation of the output signal. It has no statistical meaning. Its presence can sometimes be reduced by a careful design of all the individual sensor parts, but cannot be eliminated. It is a rather complex phenomenon, probably due to the aging effects of the microscopic constituents of the sensing material.

EXAMPLES
Metallic and Semiconductor Thermistor

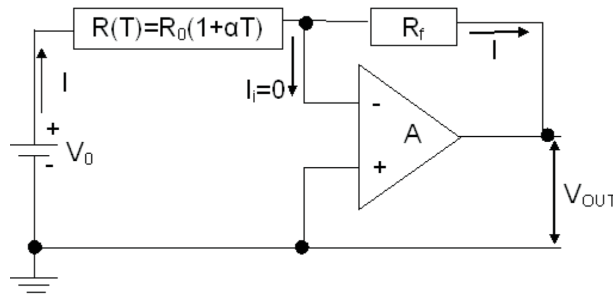

Figure 3. Schematic design of thermistor signal read-out circuit.

As a first example, let us consider a metallic thermistor inserted in fig. 3, whose resistance is, in a first approximation, expressed as: $R(T)=R_0(1+\alpha T)$. R(T) is the resistance of a PTC thermistor at a given temperature T, R_0 is the resistance at T_0, and I represents a suitable DC (or AC current), while A is the constant gain of a low noise amplifier, operating in a suitable bandwidth. Let us suppose that the injected current I does not induce, through the heating process, a detectable change of the resistance value.

In order to allow the resistance measurement, the current injection is obtained in the circuit represented in fig. 3, by applying a voltage V_0. This current, due to the virtual ground condition determined by the circuit configuration (very high input impedance), will cross the feedback resistor R_f and determine an output voltage. In this example M and Y_j (j=1,2,3) are the quantities:

$$M = T; Y_1 = R, Y_2 = I, Y_3 = V_{OUT}. \tag{4}$$

The Sensitivities can then be written as:

$$^{i}S = \frac{dY_1}{dM} = \alpha R_0 \tag{5}$$

$$^{T}S = \frac{dY_2}{dY_1} = -V_0 \frac{1}{R(T)^2} \tag{6}$$

$$^{A}S = \frac{dY_3}{dY_2} = -R_f. \tag{7}$$

The Overall Amplifier Sensitivity can be expressed as:

$$^{A}S_0 = {}^{A}S * {}^{T}S * {}^{i}S = \frac{\alpha * V_0 * R_f}{R_0 * (1 + \alpha T)^2} \tag{8}$$

and finally the Resolution is given by:

$$\Delta T = \frac{V_{noise}}{^{A}S_0}. \tag{9}$$

This means that in order to determine the temperature resolution, the sensitivity should be estimated and noise measurement performed at the output of the circuit.

It is worth mentioning that the overall sensitivity can be modified by changing both the value of the polarization current I and the amplification value A. As a particular case, when $I = 1\mu$A and A= 10^6, the product of I and A is equal to 1, so that the Overall Sensitivity coincides with the Internal Sensitivity divided by R(T).

All the changes in I and A should be done in order to have negligible self-heating of the thermistor, and an amplifier must be selected having a noise as low as possible in order to obtain an optimal resolution value for the determination of small temperature changes.

A second example is the case of a negative temperature coefficient (NTC) thermistor, such as a semiconductor, characterized by:

$$R(T) = R_0 \cdot e^{-\beta T} \qquad {}^{i}S = \frac{dY_1}{dM} = -\beta \cdot R(T). \tag{10}$$

The Overall Amplifier Sensitivity ^{A}S$_0$ can be expressed as:

$$^{A}S_0 = {}^{A}S * {}^{T}S * {}^{i}S = \frac{-\beta * e^{\beta T} * V_0 * R_f}{R_0} \tag{11}$$

and the Resolution is given by:

$$\Delta T = \frac{V_{noise}}{\prod^{i} S_i} = \frac{V_{noise}}{^{A}S_0}. \tag{12}$$

2. Fundamentals Devices

The MOSFET, the most important microelectronic device, can be reduced in dimension to reach a minimum feature size of 0.1 micron but even lower dimensions (0.05 microns) are foreseen, as demonstrated by recent advanced experiments.

Relevant for our discussion is the genesis of the sensitivity behaviour in a class of devices all generated from the well known MOSFET structure (ISFET and GASFET). In particular, the influence of charges into the gate oxide on the threshold voltage and MOSFET behaviour under shrinking conditions will be discussed.

The MOSFET operation

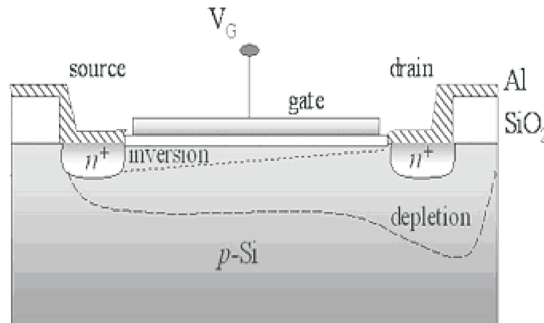

Figure 4. Cross-sectional view of a n-channel MOSFET.

The charge control equation related to this device in the quasi-linear region is approximately given by:

$$I_{DS} = \mu_n C_{ox} \frac{W}{L}[(V_{GS} - V_T)V_{DS} - \frac{V_{DS}^2}{2}] \tag{13}$$

where

- C_{ox} = oxide capacitance
- V_{DS} = dc drain-source voltage
- V_T = threshold voltage
- V_{GS} = gate voltage
- μ_n = inverted channel electrons mobility.

In the saturation region, at and above the pinch-off point, neglecting the effective channel length change due to the V_{DS} value, due to the condition $\partial I_{DS}/\partial V_{DS} = 0 (thus V_{DS} = V_{GS} - V_T)$, this equation becomes:

$$I_{DS} = \mu_n C_{ox} \frac{W}{L} [(V_{GS} - V_T)^2]. \tag{14}$$

Considering the above two equations, it is possible to derive the two transconductance expressions, $g_{m,LIN}$ and $g_{m,SAT}$ as follows:

$$g_{m,LIN} = \frac{\partial I_{DS}}{\partial V_G} = \mu_n C_{ox} \frac{W}{L} V_{DS} \tag{15}$$

$$g_{m,SAT} = \frac{\partial I_{DS}}{\partial V_G} = \mu_n C_{ox} \frac{W}{L} (V_{GS} - V_T). \tag{16}$$

It is worth pointing out that g_m has the same meaning as the output current-input voltage gate sensitivity (S).

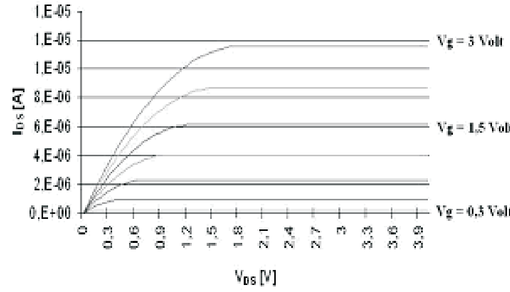

Figure 5. $I_{DS} - V_{DS}$ characteristic with V_{Gn} as input parameter($V_{Gn} > V_{Gn-1}$).

From the transconductance expressions we see that the first (eq. 15) is linear with V_{DS} and the second (eq. 16) is related to both MOSFET gate voltage V_{GS} and its threshold voltage V_T. In both cases C_{ox} plays an important role. In fact in order to increase the sensitivity, the gate oxide thickness should be as thin as possible. $g_{m,SAT}$, according to equation 16, depends on V_T and it is known that V_T depends on V_{FB}, the flat band voltage, according to:

$$V_T = V_{FB} + V_C + 2|\Phi_P| + \frac{1}{C_{ox}} \sqrt{2 \varepsilon_S q N_a (2|\Phi_P| + V_C - V_B)} \tag{17}$$

where

- V_C= voltage applied at drain
- Φ_P= potential in a doped region
- ε_S= relative dielectric constant
- N_a= acceptor atomic density
- V_B= voltage applied at substrate.

Influence of charges into the oxide layer in a MOS system

It is important to briefly recall the influence of a given charge distribution present in the oxide on V_{FB}, and, as a consequence, on V_T [2]. If

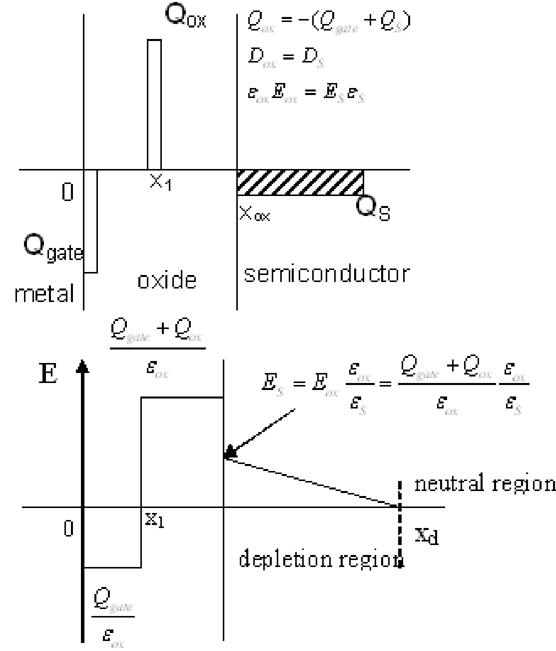

Figure 6. example of sheet of charge and approximate plot of the electric field in the Q_{ox} in the oxide layer MOS system.

a charge distribution $\rho(x)$ is present in the oxide, V_{FB} is given by:

$$V_{FB} = \Phi_{MS} - \frac{Q_f}{C_{ox}} - \frac{1}{C_{ox}} \int_0^{x_{ox}} \frac{x\rho(x)}{x_{ox}} dx \tag{18}$$

where

- Φ_{MS}= metal semiconductor work functions difference
- Q_f= fixed charge at the $SiO_2 - Si$ interface.

In fact the effect of any oxide charge is to shift the flat band voltage from its value related to the ideal case (absence of charges into the oxide). If this charge is stable, the shift induces a stable change of the threshold voltage V_T. If this charge is *not stable*, the transconductance value will not be stable and, as a consequence, the I_{DS} will experience

an unwanted change that may affect the useful signal in real operative conditions.

On the other hand, *fixed (stable) charges* into the oxide may be tolerated, and their influence overcome, if a calibration procedure is considered before any estimation of the MOSFET output.

In order to give an example of oxide charge induced MOS behaviour, let us consider the case of fig. 6 where a sheet of charge Q_{ox} is inside the oxide at $x_{1,}$ and where the corresponding electric field is drawn according to Gauss' law:

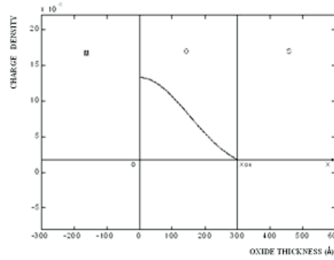

Figure 7. Example of charge half Gaussian distribution inside the oxide layer of a MOSFET structure.

Due to the electric field presence in the semiconductor, Q_{ox} will influence its flat band voltage. It is possible to derive, from simple considerations related to electrostatics, that the V_{FB} variation ΔV_{FB}, when a charge Q_{ox} is in the oxide at position x_1, is given by [2]:

$$\Delta V_{FB} = -\frac{Q_{ox} x_1}{C_{ox} x_{ox}}. \tag{19}$$

This means that if $x_1 = x_{ox}$, ΔV_{FB} will be equal to $-Q_{ox}/C_{ox}$, as expected.

On the other hand if $x_1 = 0^+$ (in other words, if Q_{ox} is just inside the oxide at $x = 0^+$), $-Q_{ox}$ will fully compensate the positive charge, and ΔV_{FB} will be zero. In fact the electric field into the silicon will be about zero and Q_{ox} will not influence the quiescent point.

It is worth noting that if Q_{ox} is moved just outside the oxide layer (for instance at $x = 0^-$), then ΔV_{FB} will be different from zero because the situation will correspond to a positive voltage directly applied to the gate by a virtual metal gate represented by the sheet of charge of intensity $+Q_{ox}$. As an example, if the oxide charge can be represented by half of the Gaussian distribution, as follows

$$\rho(x) = \frac{1}{\sigma\sqrt{2\pi}} exp[-\frac{x^2}{2\sigma^2}], \tag{20}$$

the flat band voltage contribution will be given by:

$$\Delta V_{FB} = \frac{\sigma}{C_{ox} x_{ox} \sqrt{2\pi}} \{exp[-\frac{x^2}{2\sigma^2}] - 1\}. \tag{21}$$

The ISFET operation

In principle the ISFET is derived from a MOSFET, where the metal is replaced by the couple solution-reference electrode and where a CIM (Chemically Interactive Material) is deposited on the SiO_2, the gate oxide.

The purpose of the CIM is to attract ions present in the solution; the incorporated ions represent an equivalent charge near the SiO_2 and it is equivalent to a voltage applied to the gate. In particular cases the CIM can be the SiO_2 itself or a thin film of Si_3N_4 or other insulators. As an example, in order to obtain an ISFET sensitive to K^+ ions in solution, valynomicine may be utilized as a CIM.

An approximate expression for the V_{FB} of an ISFET is:

$$V_{FB} = E_{ref} - \Delta\phi_i - (\phi_0 + \frac{RT}{F} \ln a_i) - \phi_{Si} - \frac{Q_{SS}}{C_{ox}} - \frac{1}{C_{ox}} \int_0^{x_{ox}} \frac{x\rho(x)}{x_{ox}} dx \tag{22}$$

$$E_{ref} = \mu_+^{El} - \mu_+^{met} \tag{23}$$

where

- $\Delta\phi_i$= correction factor
- ϕ_0= standard potential of the oxide-electrolyte interface
- a_i= ion activity of the electrolyte
- ϕ_{Si}= silicon work function
- Q_{SS}= charge of the surface states
- $\int_0^{x_{ox}} \frac{x\rho(x)}{x_{ox}} dx$= oxide charge.

At this point it is worth mentioning that the space charge regions present from the reference electrode up to the semiconductor show different electric fields, and as a consequence, different potential drops. The contribution of all of them determines the operating point (QP) of the system.

Around this point any change of the electrolyte concentration would change the I_{DS} current by a certain sensitivity value. Once the noise at QP is measured, then the resolution at QP may be evaluated by

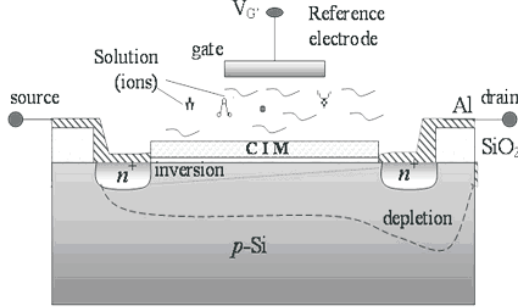

Figure 8. cross sectional view of an ISFET in a solution with the reference electrode.

$R_{QP} = V_{N,QP}/S_{QP}$, where $S_{QP} = \partial I_{DS}/\partial C_{onc}$ and all quantities are dependent on the quiescent point (QP).

Moreover it is important to stress that any change of one of the above mentioned space charge regions, either in solids or in liquids, will yield, as final effect, a change of the output current of the system.

Finally we observe that changes of the I_{DS} can only come from changes related to what is in between the gate and the semiconductor. Charges out of the gate have no influence on the system. This observation will prove useful in understanding the GASFET operation.

Essential is the presence of the reference electrode, which means an electrode whose potential is solution-independent and should also be temperature independent, at least in a specific range around the QP.

Any charge change occurring only "between" the reference electrode and the semiconductor is a candidate for a change of I_{DS}. In particular one of the most important points is the surface potential at the oxide-solution interface (φ_0) if no CIM is present, or the surface potentials between the CIM and the solution and the potential between the SiO_2 and the CIM, in the presence of a given CIM. The ISFET operation may be represented by the following "changes-flow" which may be considered as superimposed on the quiescent point determined by the reference electrode potential:

$$\Delta\varphi_{0SiO_2-El.} \rightarrow \Delta V_{FB} \rightarrow \Delta V_T \rightarrow \Delta I_{DS} \rightarrow \Delta V_{out} \tag{24}$$

$$\Delta\varphi_{0CIM-El.} \rightarrow \Delta\varphi_{SiO_2} \rightarrow CIM \rightarrow \Delta V_{FB} \rightarrow \cdots \tag{25}$$

In the absence of a given CIM the device shown in fig. 8 may become the well known pH sensor.

It is worth mentioning that a variety of insulators may be utilized, as well, for pH measurements, such as oxides of Ti, Ta, Al, Ir. All of

them, due to their different permittivity values, give rise to different sensitivities for the ISFET and also for the GASFET.

The GasFET operation

GasFETs are devices similar to MOSFET, and are able to show a certain sensitivity to volatile compounds. The intrinsic sensitivity mechanism is based on the possibility of generating either a positive or negative charge to be deposited in the vicinity of the SiO_2-CIM interface or even on the top of the CIM. A conductive gate must be present in order to get the correct operating point of the FET structure and an air gap must be present too between the CIM and the gate in order to permit the gas to flow.

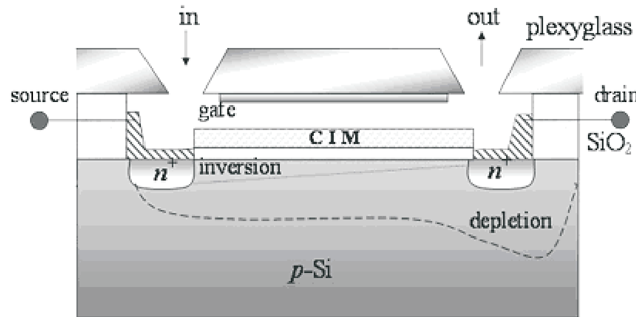

Figure 9. cross sectional view of a GASFET where the CIM is deposited on the SiO_2 layer.

For example the Pd gate MOSFET is sensitive to hydrogen due to the catalytic behaviour of palladium (very few metals are transparent to a given gas at standard pressure and temperature). The diffusion of hydrogen atoms at the Pd-SiO_2 interface and, in a first approximation, the consequent local change of the work function of the Pd-H structure, induces a change in V_{FB} and, as a consequence, in the I_{DS}, with a certain degree of sensitivity.

The necessity to have an air gap with the aim of allowing the volatile compounds to enter and leave the system, has an influence on the overall sensitivity. In fact it becomes reduced due to the presence of additional capacitors in series with that due to the SiO_2 layer. The total capacitance is made up by the presence of C_{ox}, due to the SiO_2 layer, C_{CIM},

due to the CIM layer and C_{air} due to the air gap:

$$C_{TOT} = \frac{1}{\frac{1}{C_{ox}} + \frac{1}{C_{CIM}} + \frac{1}{C_{air}}} \tag{26}$$

$$g_{m,SAT} = \frac{\partial I_{DS}}{\partial V_G} = \mu_n C_{TOT} \frac{W}{L}(V_G - V_T). \tag{27}$$

Due to the fact that C_{air} is small enough, we get in a first approximation:

$$C_{TOT} = \frac{C_{ox} C_{air} C_{CIM}}{C_{air} C_{ox} + C_{ox} C_{CIM} + C_{CIM} C_{air}} \approx C_{air}. \tag{28}$$

In order to have a large $g_{m,SAT}$ a high C_{air} value should be used or, in other words, the air gap should be as small as possible.

Two different situations are possible as far as the GasFET architecture is concerned.

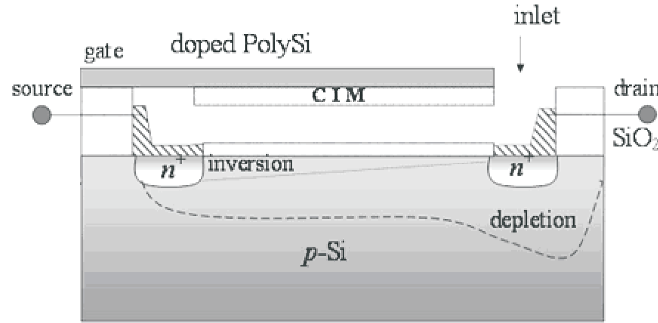

Figure 10. cross sectional view of a GASFET where the CIM is deposited underneath the gate.

Considering the two architectures of figs. 9 and 10, we have two kinds of sensitivity: one is related to the ratio of the output current variation ΔI_{DS} with respect to ΔV_G; the other is related to the ratio of the output current variation ΔI_{DS} with respect to the equivalent voltage change due to a charge variation occurring on behalf of the adsorbing CIM. The configuration of fig. 9 is certainly preferred to that of fig. 10, because in fig. 9 the charge variation at the CIM level is closer to the SiO_2 layer, when compared to the situation occurring in fig. 10. As a consequence, a greater effect will be induced on the depletion-inversion regions of the silicon underneath the SiO_2.

MOSFET shrinking

It is not obvious that the sensor technology takes advantage of the integrated transistor shrink (ITRS) trend. In fact actual MOSFET dimen-

sions offered by microelectronic technology are already even too small for most of the sensor applications.

First, the decreasing supply voltages tend to reduce the dynamic range of analog circuitry, unless this is compensated for by a substantial increase of power dissipation. Next, device miniaturization enhances, rather than reduces, 1/f noise. Finally, the very high cost of silicon real estate after a deca-nanometer process could become incompatible with the requested size of on-chip sensors.

According to the scaling rules, the MOSFET transconductance is expected to remain constant if both the lateral and vertical device dimensions are reduced by the same scaling factor λ. For a short-channel MOSFET, the saturation current I_{DSAT} may indeed be expressed as

$$I_{DSAT} = WC_{ox}(V_{GS} - V_T - V_{DSAT})v_{sat} \tag{29}$$

where W is the device width, C_{ox} is the oxide capacitance per unit area, V_{GS} is the gate-source voltage, V_T is the threshold voltage, V_{DSAT} the saturation voltage and v_{sat} is the carrier saturation velocity. The device transconductance turns out to be

$$g_m = WC_{ox}[1 - (dV_{DSAT}/dV_{GS})]v_{sat} \tag{30}$$

and, under the assumption that (dV_{DSAT}/dV_{GS}) is roughly constant for a given ratio V_{DD}/V_T , it turns out that W scales with λ and $C_{ox} = (\kappa \quad \varepsilon / t_{ox})$ with $1/ \lambda$, regardless of the voltage scaling factor. Thus, the MOSFET transconductance is expected to basically remain constant through several technology generations, provided high-κ dielectrics under development compensate for the non-scalability of the oxide thickness t_{ox}. On the other hand, the transconductance per unit width (g_m/W) is expected to increase by the scaling factor λ.

Connected with the transconductance scaling rules is the behaviour of the thermal noise, and the mean square value of the current $<i_d^2>$ in saturation reads: $< i_d^2 > = 4KT \ \gamma g_m$. Here γ is a factor which, within a simplified MOSFET model, equals 2/3, but it may become larger under strong non equilibrium conditions, where the average energy of the carriers increases well above (3/2)KT. Due to the insensitivity of the device transconductance to the scaling factor, the thermal noise is expected to stay nearly constant as the device size is scaled down. The major problem comes instead from the flicker noise, otherwise referred to as the 1/f noise, which increases inversely with the gate area. The flicker noise is modeled as a voltage source of value: $< v_g^2 >= K/(WLC_{ox}f)$, in series with the gate. Here K is a process-dependent constant.

Therefore the flicker noise is expected to grow with γ as the device size is scaled down. In deep submicron MOSFETs the corner frequency at which thermal noise equals flicker noise may be as large as 100 MHz, indicating that, at low frequency, 1/f noise is the most severe noise source which affects sensor performance.

When the available gate area is further reduced and the number of devices may increase, another crucial point is the complexity of the deposition of a suitable and possibly different chemically interactive material (CIM) on their gates. This problem may have a solution in those cases where different kinds of CIMs are mixable without altering their individual properties. In fact with only one deposit, if the gate areas are sufficiently small most of the gates will be covered by different compositions of CIMs. This process would allow the easy fabrication of single chip electronic noses with the possibility of a high degree of redundancy.

3. Thermopiles

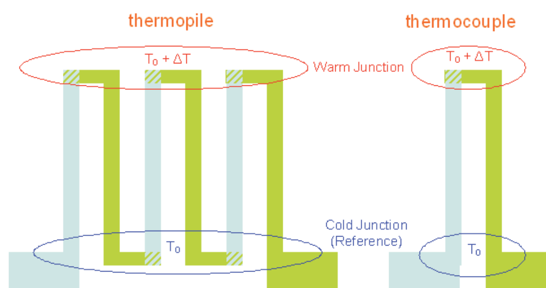

Figure 11. Schematic design of Thermocouple and Thermopile.

Thermopiles are considered temperature sensors and are fabricated incorporating a number of thermocouples. Each thermocouple is formed by a couple of different materials (Metal1-Metal2, Metal-Semiconductor, Semiconductor-Semiconductor) and responds to a temperature difference localized between the two junctions (cold junction and warm junction), see fig. 11. One of the two junctions can be considered the reference one.

During operation the voltage developed at the thermopile output is proportional to the thermoelectric power of each of the two different materials and to the temperature difference between the warm and cold junction (Seebeck effect).

When constituted of metals, thermopiles exhibit a very low noise, in particular only thermal noise if the voltage amplifier used for signal amplification has a very high input impedance.

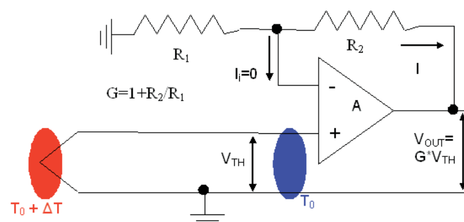

Figure 12. Schematic design of thermocouple or thermopile signal read-out.

Thermopiles can be deposited through thermal evaporation or even sputtering on either hard or soft substrates.

A thermopile can also be used as a chemical sensor if one of the two materials is a catalytic metal for a given volatile compound. In this case it is necessary to keep the warm and cold junctions at constant temperature. During absorption of the volatile compound on behalf of the catalytic material the thermoelectric power may change, giving rise to an output voltage which can be related to the concentration of the volatile compound. A typical example is the thermopile as hydrogen sensor, where one of the two materials is palladium, a standard hydrogen catalyzer.

4. Kelvin Probe

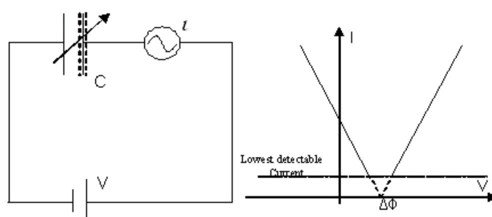

Figure 13. Schematic design of Kelvin Probe circuit and its signal output.

The importance of surfaces has grown along with the development of chemical sensors in recent years, due to the interaction between a given volatile compound and the surface of a chemically interactive material.

The Kelvin Probe technique allows measurement of the Work Function of a given surface, not only in stationary conditions but also during absorption – desorption processes.

In its simple form the Kelvin Probe is shown in figure 13, where the test plate is left fixed while the other plate of the capacitor can

be mechanically moved in different ways, in particular, as one possible example, with a piezoelectric system.

According to electromagnetic theory, any time a charge capacitor changes its value a displacement current is generated, expressed as $I = dQ/dt = CdV/dt + VdC/dt$.

The experiment is conducted measuring the current corresponding to different voltages (positive and negative) applied to the capacitor. Since the overall voltage applied to the capacitance is $V - \Delta\Phi$ the displacement current is given by: $I = (V - \Delta\Phi)dC/dt$.

A plot of current vs. voltage allows the $\Delta\Phi$ to be determined as the intersection of the current amplitudes on the X-axis.

5. Bulk Acoustic Waves

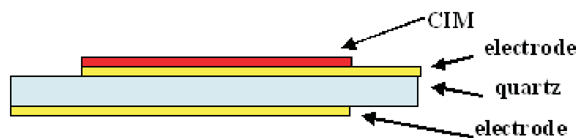

Figure 14. Quartz resonator as microbalance for chemical sensing.

A schematic diagram of a bulk acoustic wave (BAW) chemical sensor is composed of a BAW piezoelectric resonator with one or both surfaces covered by a membrane (CIM) (fig. 14).

The BAW structure is usually connected to a suitable amplifier to form an oscillator whose resonant frequency is related to both the physical and geometrical characteristics of the device.

Any change in the physical properties of the membrane due to adsorption or absorption of chemical species from either the gas or liquid phase affects the resonant frequency of the structure.

The resonator is usually made of quartz and both longitudinal and shear modes can be used. As to the quartz, crystallographic cuts showing a highly stable temperature operation dependence are carefully selected in order to improve the possibility of obtaining satisfactory resolution values.

6. Surface Acoustic Waves

Surface acoustic wave (SAW)-type chemical sensors exploit the propagation loss of the acoustic waves along layered structures consisting of at least a substrate covered by the CIM.

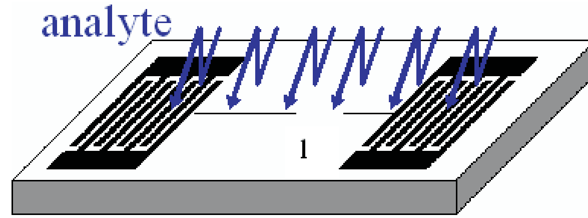

Figure 15. Basic structure of a SAW chemical sensor.

Changes produced by the measurand on the properties of the CIM can affect both the phase velocity and the propagation loss of the acoustic wave. There are examples of SAW sensors based on the measurements of the changes in the phase velocity.

A SAW device is configured as a delay line and fed by a radio frequency signal. Any change in the velocity Δv is detected as a change $\Delta\Phi$ in the phase delay of the wave, thanks to a phase detector that gives a voltage proportional to the difference of phase between signal input and output.

$$\varphi = 2\pi\frac{1}{\lambda} = 2\pi\frac{lf}{v} \tag{31}$$

$$\Delta\varphi = 2\pi lf \cdot \Delta(\frac{1}{v}) = -\varphi_0\frac{\Delta v}{v}. \tag{32}$$

7. Natural and Artificial Olfaction

In the last decade much effort has been oriented to the fabrication of artificial olfaction machines able to determine chemical images (also odor images) of complex volatile compounds. Today many different electronic noses and tongues are available for odor detection and classification and for the creation of chemical images of liquids.

Characteristics comparison of natural and artificial olfaction	
Natural olfaction	Artificial Olfaction
■ Receptors: -Non selective -Ultrahigh Redundancy(10^8) -Biochemical transduction signal: pattern of spikes. ■ Sample Delivery: -Actuation of sniffing -Two sources of odor (outside and inside) ■ Signal processing: Data synthesis ■ Data analysis: -Ultra Wide Database -Drift compensation -High integration with other senses	■ Sensors: -Non Selective -Low Redundancy (10) -Chemical transduction signal: steady signal ■ Sample Delivery: -Continuous sniffing -A source of odor (outside) ■ Signal processing: One sensor–one signal ■ Data analysis: -Limited database -Poor drift compensation -Integration with other instruments

These systems are formed by a number of cooperating individual non-selective sensors, whose outputs are processed to form chemical images or, in the presence of odors, olfactory images.

Natural olfaction does not give analytical information about the inhaled air, but rather it provides signals to the brain in order to get, at the perception level, a qualitative description of the sniffed air. Also natural olfaction utilizes a huge number (millions) of non selective receptors which show sensitivity to thousands of different odors. The artificial olfaction system has a smaller number (from 5 to 50) of sensors and, after a suitable data analysis technique, it is possible to obtain images of the volatile compound clusters present in the environment. The sensors used most for artificial nose applications are those based on quartz micro-balances, operating at room temperature, or those employing metal oxide semiconductor materials such as SnO_2 (operating in the temperature range (200-500) $^\circ$C, doped with different catalysts, in order to give a higher sensitivity toward gasses in the detection processes.

Varieties of polymers are also employed as sensitive material for electronic nose applications, and the operating temperature may reach about 100 $^\circ$C. In the case of quartz microbalance-based sensors a large role is played by the chemically interactive material (CIM) on which it is deposited. A rather efficient room temperature operating CIM is the metal-porphirin, by which it is possible to construct varieties of nostrils, just changing the type of coordinated metal. Interesting metals success-

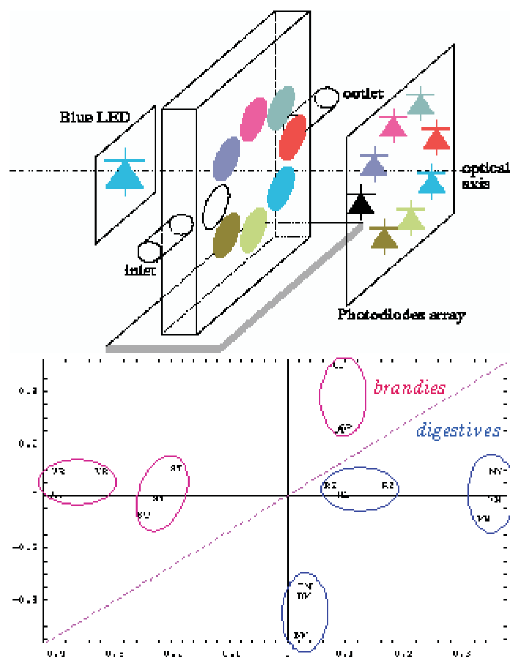

Figure 16. Opto-nose and multi-component analysis of nose output.

fully employed are: cobalt, zinc, copper, magnesium, iron, etc. Fig. 16 shows an opto-nose and the principal components analysis result related to the discrimination skin to distinguish brandies and digestives, while fig. 17 shows the typical multi-component analysis data of a nose output [3].

Future perspectives for the electronic nose research field are listed below. They concern both expected sensing and technical sensing and performance. Improvement of sensing performance of the instrument:

- Increase of both selectivity and sensitivity of the instrument towards different samples;
- Introduction of enrichment techniques of headspace sampling;
- Optimization of molecular structures towards more specific applications;
- Generation of more reproducible and long-life sensors.

Improvement of technical performances of the instrument:

- Creation of a portable nose powered by batteries, able to detect increasing concentration of gases (or odors);

Figure 17. Typical responses of the different sensors.

- Miniaturization of the instrument.

8. Optical Fibre Sensor

Figure 18. Propagation of light in a typical fibre sensor.

Optical fibres behave as wave guides for light. The original ones were made of glass but now polymeric materials are mostly used as they are cheaper than glass and metal wires.

The light can propagate along the fibre usually by totally internal reflection (TIR) as indicated in fig. 18. TIR is controlled by the angle of incidence and also by the refractive indices of the media involved in the propagation.

From Snell's Law, $\sin(\Theta_i) * n_i = \sin(\Theta_i) * n_r$. We have *TIR* when $\sin(\Theta_i) > n_r/n_i$, while we will have *refraction and reflection* when $\sin(\Theta_i) < n_r/n_i$. In practical cases properties of light, such as phase, polarization and intensity, can be modulated inside the wave guide by a given measurand, which is interacting, for instance, with a CIM lying within the penetration depth for the evanescent field of the light localized near the external guide surface.

Integrated guides can also be used as a chemical sensor. Fig. 19 shows a Mach-Zehnder interferometer where one of the two branches has been covered by palladium, a catalytic metal for H_2 [4]. The output phase change measurement determination of parts per million of H_2 has proven to be possible.

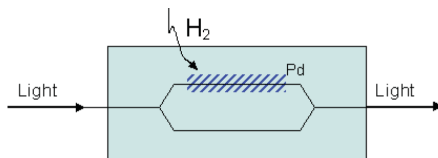

Figure 19. Mach-Zehnder Interferometer.

9. Surface Plasmon Resonance

The term surface plasmon resonance (SPR) can refer to the phenomenon itself or to the use of this phenomenon to measure biomolecules binding to surfaces. This method is now widely used in the biosciences and provides a generic approach to measurement of bio molecule interactions on surfaces.

The phenomenon of SPR is directly related to Snell's Law (see fig. 18). In fact when radiation passes to a medium with lower dielectric constant there is a critical angle beyond which the refracted beam cannot propagate in the other medium.

The decrease in reflectivity at the SPR angle (2_{SP}) is due to absorption of the incident light at this particular angle of incidence. At this angle the incident light is absorbed and excites electron oscillations on the metal surface.

It is important to understand why reflectivity is sensitive to the refractive index of the aqueous medium if the light is reflected by the gold film. This sensitivity is due to an evanescent field which penetrates approximately 200 nm into the solution [5].

The evanescent field appears whenever there is resonance between the incident beam and the gold surface and is not present when there is no plasmon resonance, that is, where the reflectivity is high.

$$\text{Total Internal Reflectance:} \qquad \sin(\Theta_i) = \frac{n_r}{n_i}. \tag{33}$$

Incident light can excite a surface plasmon when its x axis component equals the propagation constant for the surface plasmon. SPR occurs when this projected distance matches the wavelength of the surface plasmon (fig. 20).

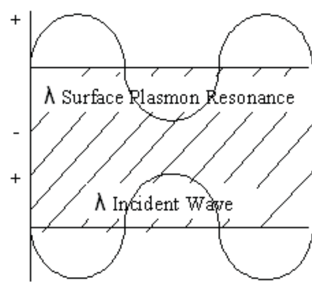

Figure 20. Condition of Surface Resonance.

Resonance cannot be excited with light incident from the air or from a medium with lower dielectric constant ($k_{SP} > k$). The refractive index of a prism reduces the wavelength to $\lambda = \lambda_0/n_P$.

A condition of resonance can be obtained by:

- $k_{SP} = k_0(\frac{\varepsilon_r \cdot \varepsilon_i}{\varepsilon_r + \varepsilon_i})$
- $k_x = k_0 \cdot n_i \cdot \sin(\Theta_i)$
- Condition of resonance: $k_{SP} = k_x$

10. Conclusions

In view of the future development of sensors driven by increasing demand for accuracy and precision, and by the opening of new fields close to the biological area (which is oriented toward nano-biosensor fabrication), it appears even more important to properly use the most relevant sensor keywords, such as: response curve, sensitivity, noise, drift, resolution, and selectivity.

The correct understanding of these words and their implications is of fundamental importance for the scientific and industrial community interested in sensor science development, since it allows the correct dissemination of both experimental and theoretic results, even if other important terms in the sensor field have not been discussed in this chapter, such as speed of response, reversibility, repeatability, reproducibility, and stability, to which some attention was paid during the presentation of this work at the ASI.

Some fundamental transducers have also been considered to explain intrinsic sensing and sensitivity mechanisms, without disregarding comments on noise which are fundamental to the determination of resolution.

References

[1] A.D'Amico, C.DiNatale. A contribution on some basic definitions of sensors properties. *Sensors Journal, IEEE*, vol. 1, Issue 3, Oct 2001 Page(s):183 - 190

[2] R.Muller, T.Kamins, M.Chan. *Device electronic for integrated circuits* John Wiley & Sons, 3rd edition, 2003.

[3] C.DiNatale, D.Salimbeni, R.Paolesse, A.Macagnano, A.D'Amico. Porphyrins-based opto-electronic nose for volatile compounds detection, *Sensors and Actuators B* 65 (2000) 220-6.

[4] A.D'Amico et al. Integrated optic sensor for the detection of H2 concentrations *Sensors and Actuators B* 7 (1992) 685-8.

[5] N.J. Walker. A technique whose time has come, Science 296 (2002) pp. 557–559.